Journal of Medicinal Chemistry

Article

pubs.acs.org/jmc

Structure Guided Design and Kinetic Analysis of Highly Potent Benzimidazole Inhibitors Targeting the PDEδ Prenyl Binding Site

Gunther Zimmermann,[†,‡] Carsten Schultz-Fademrecht,[§] Philipp Küchler,[†,‡] Sandip Murarka,[†] Shehab Ismail,[†,∥] Gemma Triola,[†,⊥] Peter Nussbaumer,[§] Alfred Wittinghofer,[†] and Herbert Waldmann*[,†,‡]

[†]Max Planck Institute of Molecular Physiology, Otto-Hahn-Strasse 11, 44227 Dortmund, Germany

[‡]Department of Chemistry and Chemical Biology, TU Dortmund University, Otto-Hahn-Strasse 6, 44227 Dortmund, Germany

[§]Lead Discovery Center, Otto-Hahn-Strasse 15, 44227 Dortmund, Germany

[∥]The Beatson Institute, Garscube Estate, Switchback Road, Bearsden, Glasgow G61 1BD, United Kingdom

[⊥]Institute of Advanced Chemistry of Catalonia (IQAC), Spanish National Research Council (CSIC), Jordi Girona, 18-26, 08034 Barcelona, Spain

Supporting Information

ABSTRACT: K-Ras is one of the most frequently mutated signal transducing human oncogenes. Ras signaling activity requires correct cellular localization of the GTPase. The spatial organization of K-Ras is controlled by the prenyl binding protein PDEδ, which enhances Ras diffusion in the cytosol. Inhibition of the Ras−PDEδ interaction by small molecules impairs Ras localization and signaling. Here we describe in detail the identification and structure guided development of Ras−PDEδ inhibitors targeting the farnesyl binding pocket of PDEδ with nanomolar affinity. We report kinetic data that characterize the binding of the most potent small molecule ligands to PDEδ and prove their binding to endogenous PDEδ in cell lysates. The PDEδ inhibitors provide promising starting points for the establishment of new drug discovery programs aimed at cancers harboring oncogenic K-Ras.

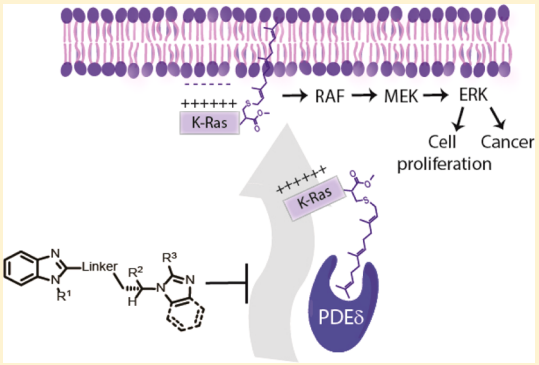

INTRODUCTION

The signal transducing Ras GTPases regulate important cellular processes such as growth, differentiation, and apoptosis.[1] Mutations in Ras-encoding proto-oncogenes that lock them in a GTP-bound active state are found in 20−30% of all human tumors.[1−3] As a result, the cycling of Ras between the active and the inactive state is impaired, and Ras signaling pathways are permanently active. Despite numerous attempts in the last decades, small molecule drugs that interfere with oncogenic signal transduction by Ras have not come within reach of the clinic.[4] Recent developments focused on the one hand on the discovery of direct Ras binders by means of fragment based compound development[5,6] and stabilization of peptide structures[7] and resulted in compounds with affinities in the micromolar range. On the other hand, a novel approach introduced small molecules that covalently bind to oncogenic K-Ras carrying the G12C mutation, which is of particular relevance in lung cancer.[8,9] Other approaches have attempted to interfere with Ras localization in the cell by means of small molecules, however the targets of the identified compounds to date remain unclear.[10,11]

The biological function of Ras proteins is linked strongly to their dynamic, subcellular localization.[12] All Ras isoforms (K-Ras4A, K-Ras4B, N-Ras, H-Ras) are farnesylated and carboxymethylated at the C-terminal cysteine residue.[1] These modifications, however, are not sufficient for stable binding to lipid double layers. While a (de-)palmitoylation cycle of N-Ras and H-Ras steers reversible binding to endomembranes, a C-terminal, polybasic lysine stretch in K-Ras4B enables stable binding to the negatively charged, cytosolic leaflet of the plasma membrane. Biochemical and cellular studies have proven the interaction between K-Ras and the prenyl binding protein and shuttling chaperone PDEδ.[13] PDEδ was initially identified as the noncatalytic δ-subunit of PDE6. Later, however, it was shown that it has an essential role in maintaining the proper cellular distribution of Ras proteins required for correct signaling.[14] In accordance with this finding, a decrease in the phosphorylation of ERK, the downstream target of Ras, signaling is observed after siRNA mediated knockdown of the *PDE6D* gene.[14,15] We have recently shown that small molecules that bind to the prenyl binding pocket of PDEδ and thereby inhibit the K-Ras−PDEδ interaction impair K-Ras signaling and the proliferation of human pancreatic ductal adenocarcinoma cells *in vitro* and *in vivo*.[16]

Here we describe in detail the structure-guided development of these highly potent K-Ras−PDEδ interaction inhibitors, which feature a benzimidazole core moiety. We provide details of the

Received: April 23, 2014

   dx.doi.org/10.1021/jm500632s | *J. Med. Chem.* XXXX, XXX, XXX−XXX

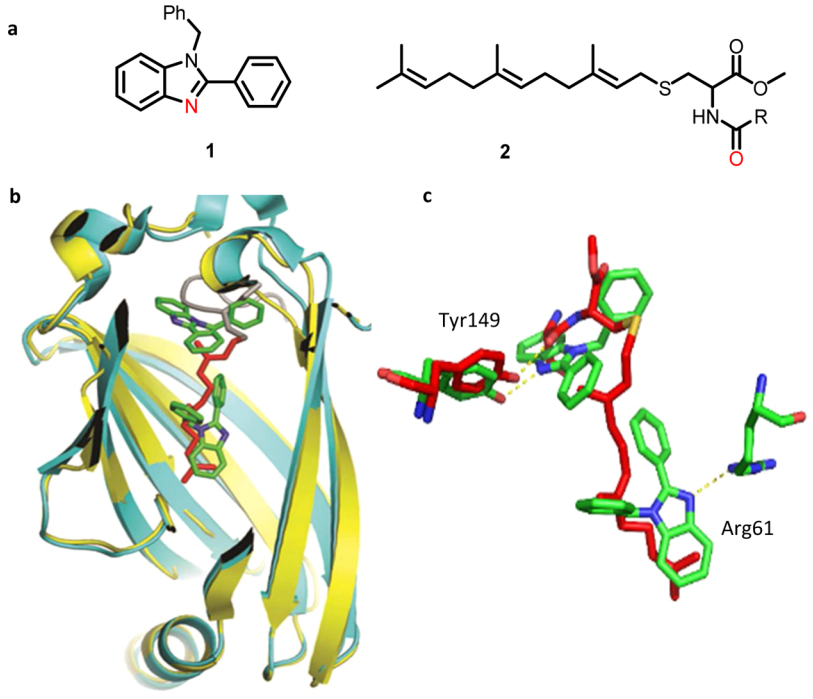

Figure 1. Overlay of the cocrystal structure of benzimidazole **1** and the farnesyl group of a C-terminal Rheb peptide with PDEδ (PDB 4JV6 and 3T5I).[16] (a) Structure of benzimidazole hit compound **1** and C-terminal, farnesylated Rheb peptide **2**; hydrogen bond acceptors for Tyr149 are highlighted in red. (b) Overall structure of inhibitor **1** (green sticks) bound to PDEδ. Overlaid is the structure with a farnesylated Rheb peptide (red). (c) Key hydrogen bonding interactions with Tyr149 (observed in both cocrystal structures) and Arg61.

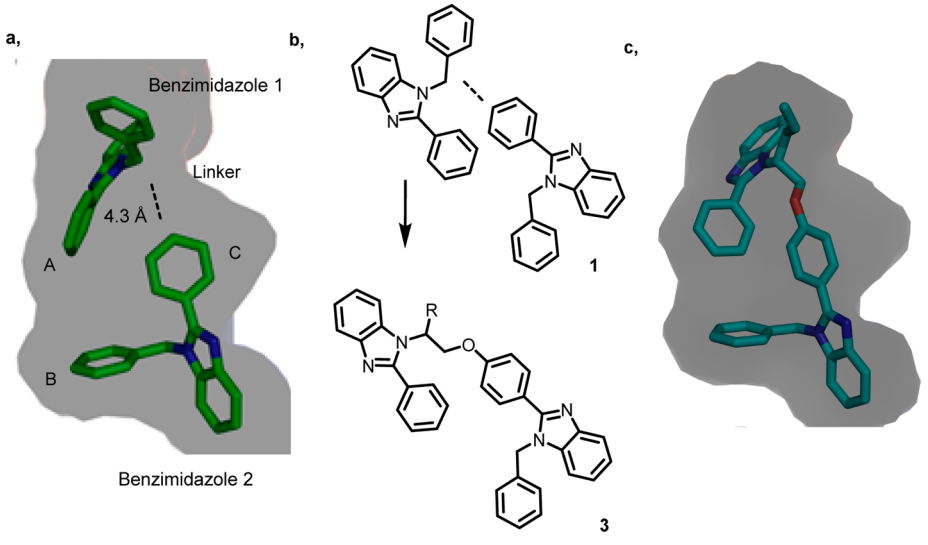

Figure 2. Design of linked benzimidazoles. (a) Surface representation of the PDEδ cavity (PDB 4JV6); the distance between linked atoms is highlighted. (b) Design of linked bis-benzimidazole ether **3**. (c) Best scoring docking pose obtained by docking a bis-benzimidazole (allyl group as R) into the crystal structure of benzimidazole fragment **1** in complex with PDEδ (PDB 4JV6).

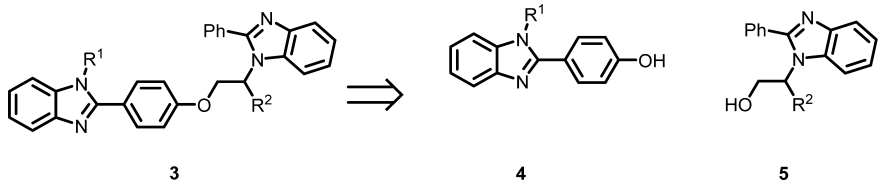

Figure 3. Retrosynthetic analysis of bis-benzimidazoles **3**.

synthesis of this PDEδ inhibitor class, describe the design of a novel hybrid pyrrole–benzimidazole PDEδ ligand class, and report the kinetic characterization of different inhibitors. Additionally we present data showing that benzimidazole

dx.doi.org/10.1021/jm500632s | J. Med. Chem. XXXX, XXX, XXX–XXX

Scheme 1. Synthesis of Ether-Linked Bis-benzimidazole 18

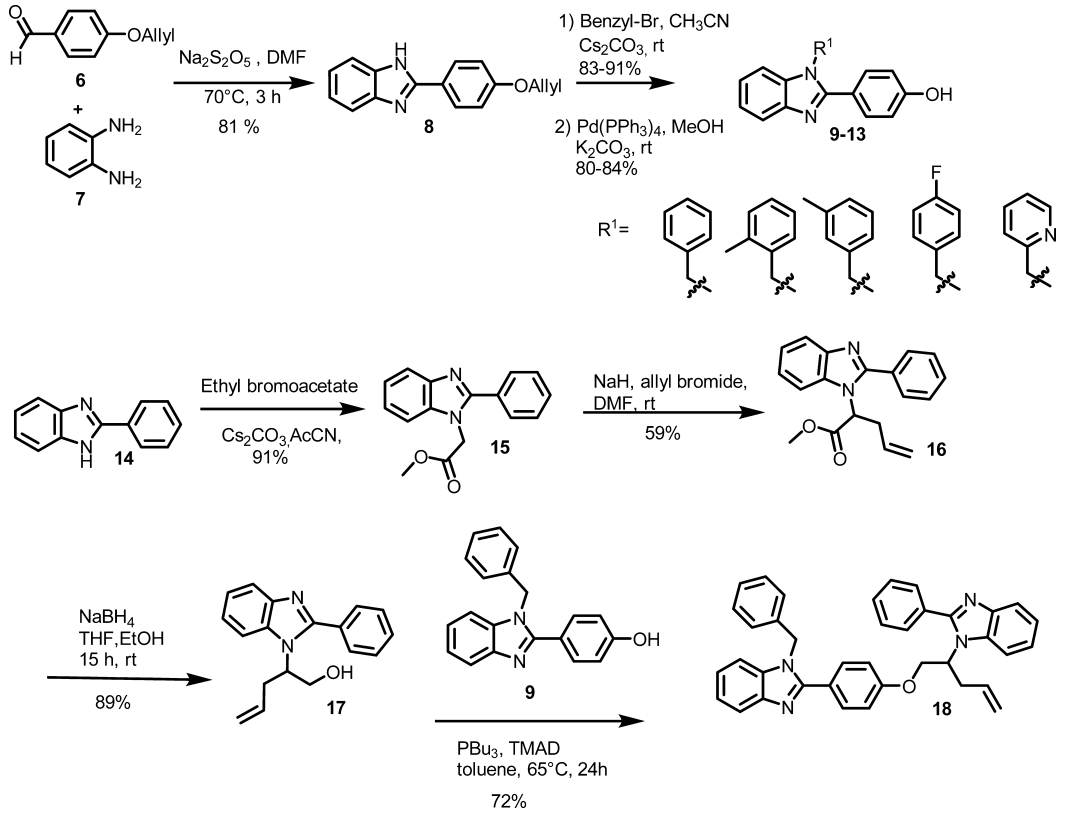

inhibitors bind to endogenous PDEδ and inhibit the Ras−PDEδ interaction in cell lysates.

RESULTS AND DISCUSSION

As previously described, screening of ca. 150 000 in house compounds by means of an Alpha Screen resulted in the identification of benzimidazole fragment **1** as an inhibitor of the interaction between PDEδ and a farnesylated K-Ras peptide (Figure 1, for $K_{D,app}$-values see the Supporting Information, Figure S1, Table S1).[16] Cocrystallization of PDEδ with compound **1** revealed that two molecules of **1** bind to the prenyl binding site of the protein.[16] Whereas one benzimidazole forms a hydrogen bond to arginine 61 deep in the binding pocket, binding to the other benzimidazole occurs via a H-bond to tyrosine 149 closer to the exit of the prenyl binding tunnel. Interestingly a H-bond to tyrosine 149 is also found in the crystal structure of PDEδ fully modified, farnesylated Rheb protein or C-terminal peptides, like **2** (PDB codes 3T5I and 3T5G, Figure 1b). Here the backbone amide between the C-terminal, farnesylated cysteine 181 and serine 180 of Rheb functions as the analogous hydrogen bond acceptor.

The binding of the two small benzimidazole fragments **1** to PDEδ was subsequently confirmed by competitive fluorescence polarization measurements, T_m shift assays, and isothermal titration (ITC) experiments.[16]

Comparison of the K_D values determined in different investigations suggested that the fragment-sized benzimidazole **1** binds slightly better than a farnesylated, labeled K-Ras4B protein (165 vs 302 nM),[16,17] In order to show high target engagement and specificity in a biological environment very high affinity compounds are desirable. It was therefore decided to link the two benzimidazole fragments identified in the cocrystal of **1** with PDEδ. Molecular modeling (Schrödinger, Maestro suite) enabled the *in silico* testing of different linkers. Phenyl rings A and B (Figure 2a) were well aligned for an edge-to-face stacking interaction, and therefore this part of the molecule was left unaltered. Phenyl ring C of the second benzimidazole on the other hand is in close proximity to the benzylic position (4.3 Å) of fragment 1 (Figure 2b). Therefore, the two fragments were connected through a short linker (Figure 2c).

In a retrosynthetic sense, the targeted bis-benzimidazoles were disconnected to phenols **4** and alcohols **5**, which can be linked by means of a Mitsunobu reaction (Figure 3).

The synthesis of benzimidazole fragments **4** commenced with commercially available phenylenediamine (**7**), which was treated with 4-allyloxy benzaldehyde (**6**) in the presence of sodium metabisulfite to give the benzimidazole **8** in 81% yield (Scheme 1). N-Benzylation of the benzimidazole followed by removal of the allyl group to liberate the phenol furnished the desired products **9**−**13** in good yield (80−84%).

Benzimidazole fragments **5** were synthesized either by an alkylation strategy or by a strategy resting on a Ugi four-component reaction (see below). Initially we focused on the synthesis of bis-benzimidazoles containing small, flexible substituents like an allyl group at position R^2 (Figure 3) to avoid clashes with the surface of the protein and to validate that indeed fragment linking leads to higher affinity. Therefore, commercially available 2-phenyl benzimidazole **14** was alkylated with ethyl bromoacetate. The intermediate ester **15** was further C-alkylated with allyl bromide and then reduced with sodium borohydride to yield alcohol **17**. Benzimidazole fragments **9** and **17** were connected subsequently by means of a modified Mitsunobu reaction with *n*-tributylphosphine and tetramethyl azadicarboxamide (TMAD)[18] (Scheme 1).

Linked allyl benzimidazole **18** bound to PDEδ with a 4−5-fold higher affinity compared with fragment **1** according to

dx.doi.org/10.1021/jm500632s | J. Med. Chem. XXXX, XXX, XXX−XXX

Table 1. Affinities of Bis-benzimidazoles Measured by Fluorescence Polarization and Change in Melting Point T_m

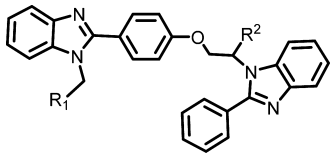

Entry	Cpd (rac)	R^1	R^2	K_D / nM	T_m shift / °C
1	**18**			39±11 [a]	19.7
2	**25**			20 ± 5	nd
3	**26**			16±2 [a]	25.8 [a]
4	**27**		CH_2COOH	870 ± 290 [a]	10.0 [a]
5	**28**		PEG-Biotin	328 ± 38	11.6
6	**29**			>2000 [a]	7.2 [a]
7	**30**		 diastereomer 1	>400	nd
8	**31**		 diastereomer 2	207 ± 42	nd
9	**32**		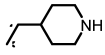	162 ± 50	nd
10	**33**			87±35 [a]	20.5
11	**34**			231 ± 28	17.4
12	**35**			251 ± 36	nd
13	**36**			191 ± 45	nd
14	**37**			474 ± 121	nd

[a] Adopted from ref 16.

fluorescence polarization measurements (Table 1, entry 1).[16] A crystal structure of linked bis-benzimidazole **18** revealed a very good overlap with the guiding benzimidazole fragment **1**[16] and an excellent overlay with highest scoring docking pose (Figure 2c). Inspection of the structure revealed that the allyl group extends into a hydrophobic cavity, which could also accommodate larger groups (Figure 4). A series of analogues with varying substituents R^1 and R^2 (Table 1)[16] was therefore synthesized following the procedure described above. Alternatively, benzimidazole

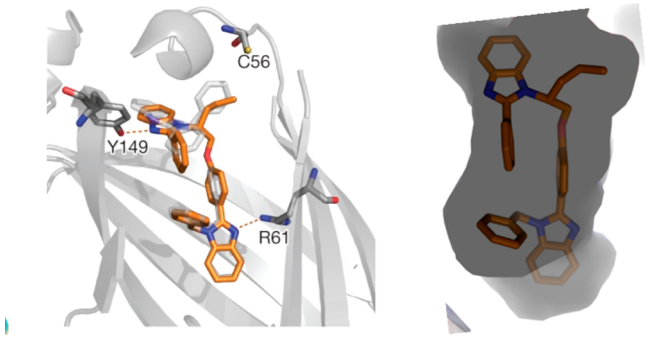

Figure 4. Crystal structure of linked bis-benzimidazole **18**. (left) Overlay of **18** (colored sticks) with guiding benzimidazole **1** (faint gray sticks). (right) View of cavity surrounding the bis-benzimidazole.

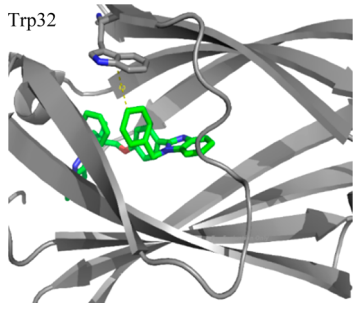

Figure 5. T-stacking interaction between benzyl moiety of compound **18** and electron-rich tryptophan.

fragments **5** were synthesized by a strategy resting on a Ugi four-component reaction (Scheme 2).[19] Briefly, commercially available Boc-protected *o*-phenylenediamine, benzoic acid, benzyl isocyanate, and the appropriate aldehyde were stirred for 36 h in MeOH to obtain the initial Boc protected Ugi product, which was then immediately deprotected and cyclized in a one-pot procedure using HCl/dioxane to yield the intermediate branched amides **23**. Boc protection of the amides, followed by reductive cleavage led to the desired primary alcohols **5**. After a modified Mitsunobu reaction (PBu_3, TMAD), the Boc-protected piperidines were deprotected using HCl/dioxane to yield the desired bis-benzimidazoles **3**.

The synthesized analogues were evaluated using previously described T_m shift and fluorescence polarization assays.[16] The allyl group of **18** was substituted with the bulkier isopropyl and cyclohexyl substituents to further explore the hydrophobic cavity around Cys56. Gratifyingly these compounds showed increased affinity (Table 1, entries 2−3), whereas introduction of a negative charge and coupling to a PEG−biotin unit resulted in lower affinities (entries 4 and 5). A Boc-protected piperidine showed only weak interaction with PDEδ, due to a presumed steric clash with the surface of the binding pocket (Table 1, entry 6). Closer inspection of the cocrystal structure between **18** and PDEδ indicated that the allyl group points toward the backbone carbonyl of Cys56 (Figure 4, left). Thus, we envisioned that an additional hydrogen bond between the ligand and the carbonyl group could be established which should lead to tighter binding. To investigate this possibility piperidine derivatives were used to replace the allyl group (Table 1, entries 7−10). Among the tested piperidines, piperidine **33** proved to be the most potent (entry 10). Unexpectedly the affinity of piperidine **33** was slightly lower than the values recorded for **18**, **25**, and **26**. However, introduction of the piperidine groups substantially increased the

dx.doi.org/10.1021/jm500632s | J. Med. Chem. XXXX, XXX, XXX−XXX

Scheme 2. Synthesis of Benzimidazole Fragments 5 via Ugi Four-Component Reaction and Fragment Linking

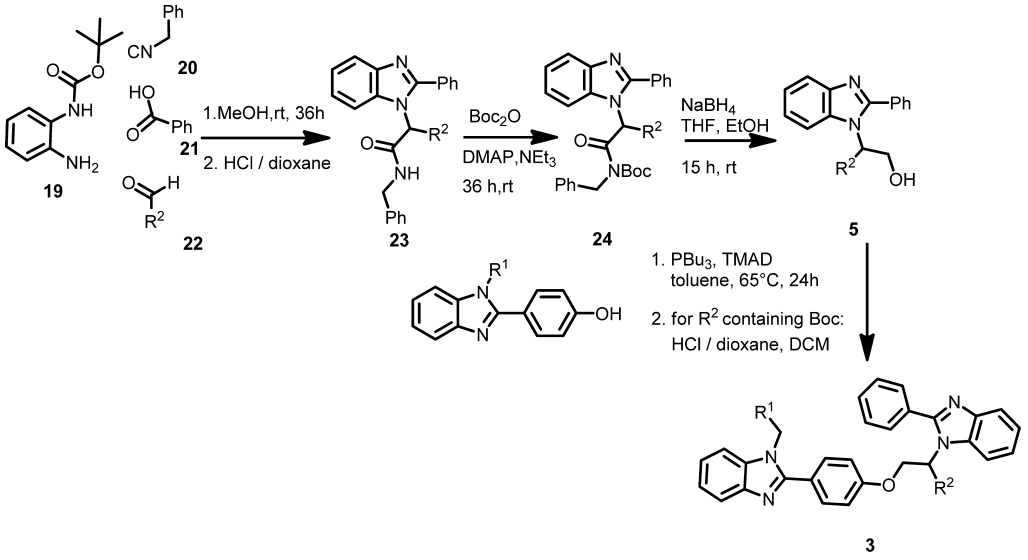

Scheme 3. Proposed Disconnection of Ester-Linked Bis-benzimidazoles (top) and Synthesis of Benzimidazole Fragments 46-48 (bottom)

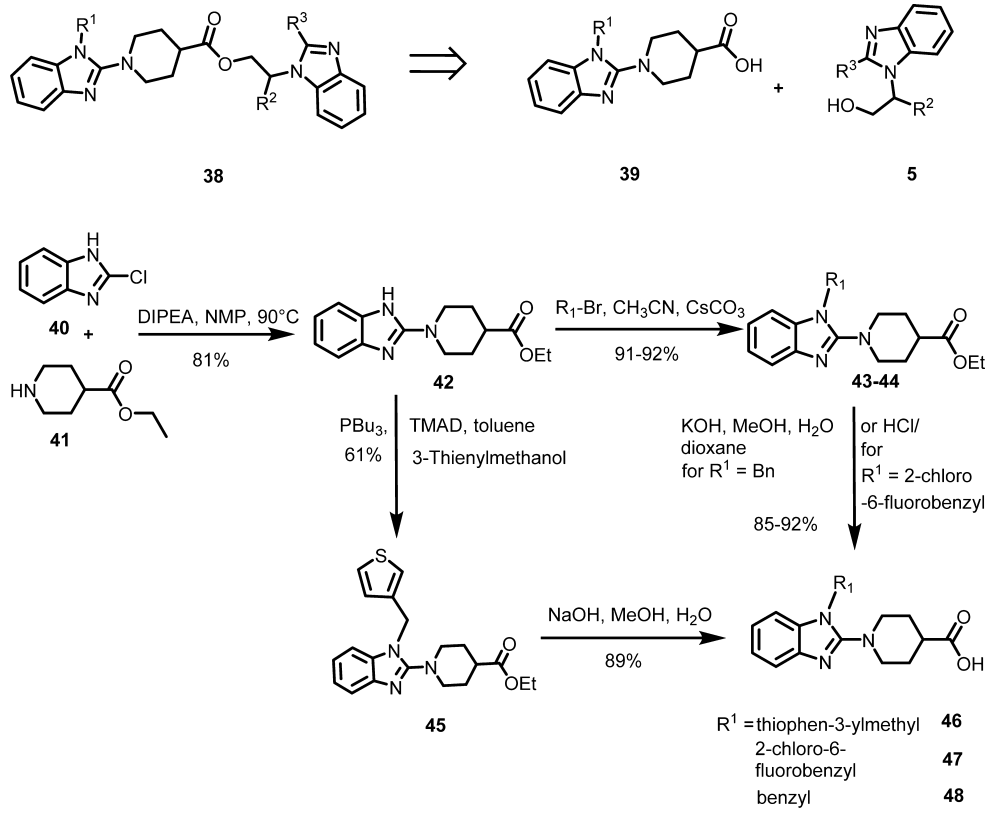

solubility of the small molecules in aqueous solutions, and the idea of installing a piperidine functionality as a hydrogen bonding donor was investigated further.

Therefore, further structural variations were conducted with the piperidine moiety in place, focused on the variation of the benzyl group. The distance between the benzyl group of benzimidazole **18** and Trp32 in the PDEδ cocrystal structure is below 4 Å suggesting that it undergoes a T-stacking interaction with the electron-rich indole (Figure 5).

Edge-to-face stacking interactions usually strongly depend on the electronic nature of the interacting aromatic moieties.[20] Therefore, electron-donating and -withdrawing groups were introduced into R^1 (Table 1, entries 11−14). Unexpectedly neither electron-poor aromatic systems (4-fluorobenzene, pyridine; Table 1, entries 11 and 12) nor electron-rich toluene derivatives (Table 1, entries 13 and 14) resulted in more potent compounds, which suggested possible clashes with the surface of the protein.

dx.doi.org/10.1021/jm500632s | J. Med. Chem. XXXX, XXX, XXX−XXX

Table 2. Affinities for Bis-benzimidazoles 49−62 with Different Linker Moieties and Different Substituents R^1 and R^2 as Determined by Means Fluorescence Polarization Measurements

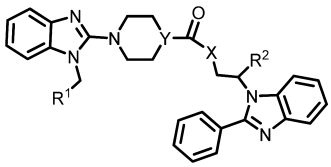

Entry	Cpd (rac)	R^1	X	Y	R^2	K_D / nM
1	**49**		O	C		10 ± 3 [a)]
2	**50**		O	C		25 ± 8
3	**51**		O	C		17 ± 3
4	**52**	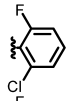	O	C		77 ± 20
5	**53**		O	C		115 ± 35
6	**54**		O	C		9±2 [a)]
7	**55**		O	C		16 ± 4
8	**56**		O	C	 diastereomer 1	18 ± 5
9	**57**		O	C	 diastereomer 2	11 ± 3
10	**58**		O	C	 diastereomer 1	13 ± 3
11	**59**		O	C	 diastereomer 2	14 ± 6
12	**60**		O	C		14 ± 5
13	**61**		NH	C		720 ± 240
14	**62**		O	N		35 ± 13

[a]Adopted from ref 16.

Based on the results shown in Table 1, we reasoned that the rigid ether linker might make the backbone carbonyl of cysteine 56 unavailable for interaction with the piperidine group. Therefore, the length of the linker moiety was increased, and the ether was replaced by a more flexible ester. In analogy to the disconnection of the ether compounds, ester-linked bis-benzimidazoles were synthesized from benzimidazole fragments, **39** and **5** (Scheme 3). Benzimidazole type fragments **39** (**46**−**48**)

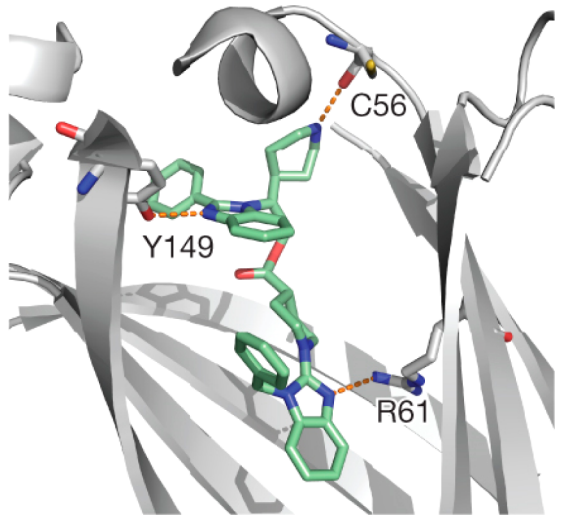

Figure 6. Cocrystal structure of linked bis-benzimidazole (*S*)-**49** and PDEδ confirms the third hydrogen bond to cysteine 56 (PDB 4JVF).[16]

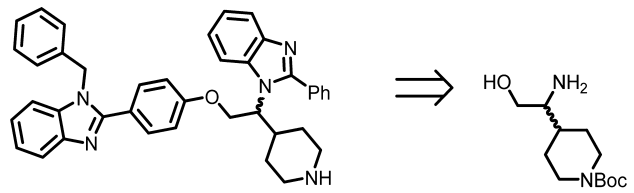

33 **63**

Figure 7. Disconnection of chiral benzimidazoles into amino alcohols.

were synthesized from 2-chlorobenzimidazole (**40**) (Scheme 3). Nucleophilic aromatic substitution with ethylpiperidine-4-carboxylate afforded ester **42** in 81% yield. The benzimidazole was then either benzylated with benzyl bromides in acetonitrile in the presence of cesium carbonate or subjected to a Mitsunobu reaction with 3-hydroxymethyl thiophene **44** (61%) in the presence of tributyl phosphine and TMAD. Cleavage of the ester under basic or strongly acidic aqueous conditions furnished carboxylic acids **46**−**48**.

Benzimidazole fragments type **39** were then linked to fragments **5** under Mitsunobu conditions (PPh_3/DtBAD). The ester compound collection was subsequently evaluated in fluorescence polarization assays. Gratifyingly, ester **49** bound to PDEδ with an affinity of 10 nM (Table 2, entry 1), while cyclohexyl and isopropyl substituted esters (R^2) displayed lower affinities (Table 2, entries 2 and 3). A cocrystal structure of (*S*)-**49** with PDEδ (Figure 6) confirmed the formation of a third hydrogen bond between the backbone carbonyl of cysteine 56 and the piperidine moiety.[16]

Consistent with the data shown in Table 1, additional electron-withdrawing substituents on the benzyl ring reduced the binding affinity and thus yielded higher K_D values (Table 2, entries 4 and 5). The replacement of the benzyl moiety at R^1 with a 3-methyl thiophene however resulted in similar affinities (Table 2, entries 6 and 7). In general, the cyclohexyl substituted benzimidazoles, which cannot form a third H-bond to cysteine 56, bind with lower affinities to the protein than the piperidines (Table 2 entries 1, 4, and 6 vs 2, 5, and 7). Replacement of the 4-piperidyl moiety at R^2 by a 3-piperidyl substituent (entries 8 and 9), a pyrrolidine (entries 10 and 11), or a 4-methylene piperidine (entry 12) did not increase affinity for the protein. However, the

dx.doi.org/10.1021/jm500632s | J. Med. Chem. XXXX, XXX, XXX−XXX

Scheme 4. Enantioselective Synthesis of Bis-benzimidazole Deltarasin, (*S*)-33, Using the Evans Azidation Approach

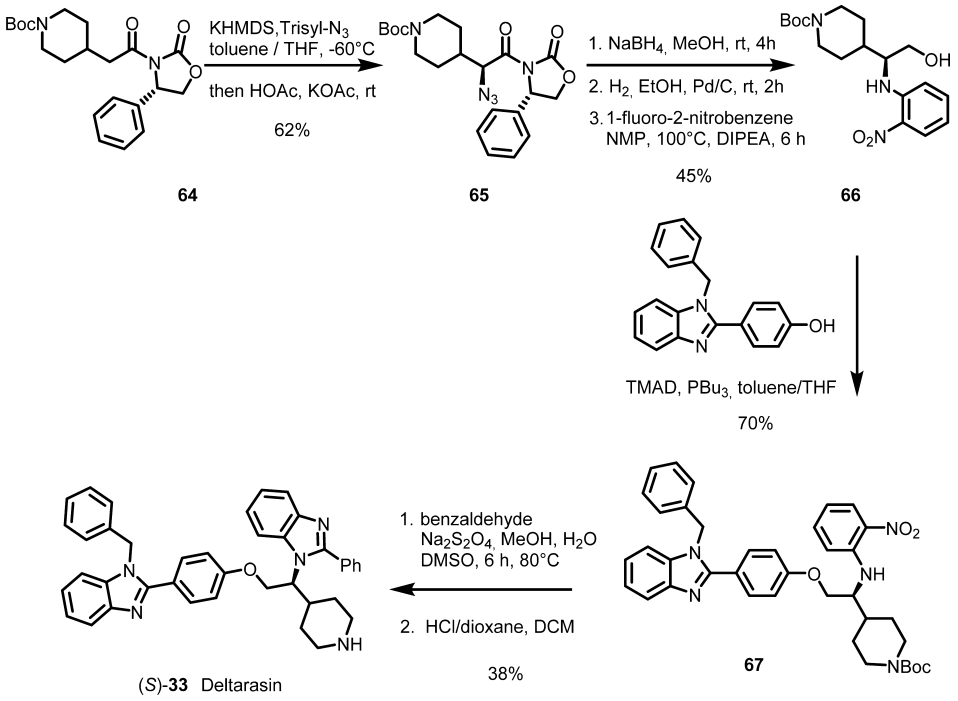

Scheme 5. Enantioselective Synthesis of Ester-Linked Bis-benzimidzoles 69−72 by Cyclization of Nitroanilines

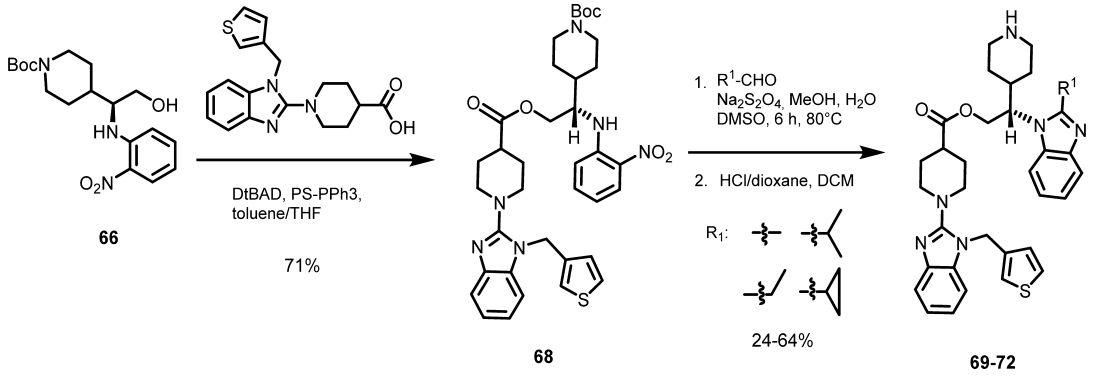

ester linked compounds in general proved to be more potent than the corresponding ethers (compare Tables 1 and 2). Due to a possible susceptibility of the ester compounds toward cleavage by hydrolases in prospective cellular investigations, the ester moiety was replaced by an amide linker. Presumably owing to the rigidity, the different hydrogen bonding properties, or a different conformation, the amide showed a lower affinity compared with the corresponding ester (Table 2, entries 6 vs 13). Replacement of the ester with a carbamate moiety however led to a similar K_D value (Table 2, entries 1 vs 14).

While the racemic ester- and ether-linked benzimidazoles displayed low nanomolar K_D values, we sought to determine which enantiomer bound with higher affinity. The enantiomers of the Boc-protected **33** and **54** were separated by preparative chiral high-performance liquid chromatography, and after Boc removal, the pure enantiomers were assayed revealing a 4−6-fold difference in potency for each pair of enantiomers.[16] To assign the absolute configuration of the most potent enantiomers, an enantioselective synthesis of **33** was performed. Compound **33** can be retrosynthetically traced back to amino alcohols (Figure 7). Since the chiral synthesis of amino acids and alcohols is well established, it was planned to assign the absolute stereochemistry according to literature precedent employing (*S*)-4-phenyl-2-oxazolidinone as a chiral auxiliary.

Hence, oxazolidinone **64**[21] was subjected to azidation with trisyl azide in a mixture of toluene/THF at −60 °C (Scheme 4). Reduction with sodium borohydride in methanol, followed by hydrogenation with Pd/C and nucleophilic aromatic substitution provided the intermediate alcohol **66**. The alcohol then underwent Mitsunobu reaction with different nucleophiles, and the nitro aniline moiety was converted into a benzimidazole via reductive cyclization using sodium dithionite. Analytical HPLC coelution studies and biochemical assays confirmed that the (*S*)-enantiomers of both the ester and ether compound series were more potent than the (*R*)-enantiomers.[16] The (*S*)-enantiomer of compound **33** was termed deltarasin, due to its proven ability to break the interaction between Ras and PDEδ in the living cell.[16]

In summary, we have identified potent bis-benzimidazoles in both ester and ether compound series. In general, the ester compounds proved to be more potent, but they are potentially susceptible to intracellular enzymatic hydrolysis. Therefore, ether compounds may be more suitable for prospective cellular experiments.[16]

dx.doi.org/10.1021/jm500632s | J. Med. Chem. XXXX, XXX, XXX−XXX

Table 3. Affinities of Ester-Linked Bis-benzimidazoles as Measured by Fluorescence Polarization

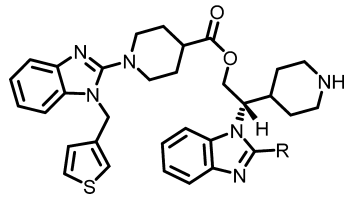

Entry	Cpd	R	K_D / nM
1	(*S*)-**54**		7 ± 3 [a)]
2	(*S*)-**69**		8 ± 2
3	(*S*)-**70**		12 ± 4
4	(*S*)-**71**		9 ± 3
5	(*S*)-**72**		35 ± 16

[a]Adopted from ref 16.

Table 4. Affinities of Smaller Bis-benzimidazoles as Measured by Fluorescence Polarization

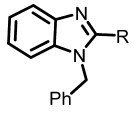

Entry	Cpd	R	K_D / nM
1	**73**	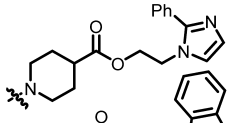	7 ± 2
2	**74**	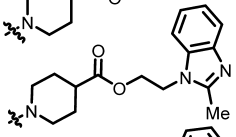	6 ± 2
3	**75**	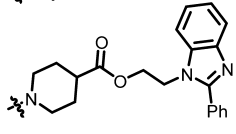	14 ± 2
4	**76**	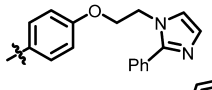	7 ± 3
5	**77**	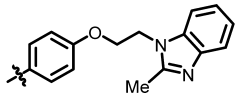	17 ± 2

Structural Simplification of Bis-benzimidazole Inhibitors. While very potent molecules were identified among the benzimidazoles, ligand efficiency, solubility, and drug likeness of the compounds still left room for improvement.[22] It was therefore envisaged to reduce the number of aromatic rings and the size of the benzimidazoles while trying to maintain potency. With the enantioselective route toward the bis-benzimidazoles in hand, initial attempts focused on replacing the 2-phenyl substituent in the ester compound series by alkyl residues

Table 5. Affinities of Benzimidazoles Featuring Michael Acceptor Functionalities To Covalently Trap Cysteine 56[a]

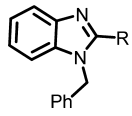

Entry	Cpd	R	K_D / nM
1	**78**	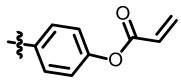	82 ± 7
2	**79**	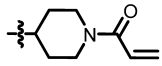	>1000
3	**80**	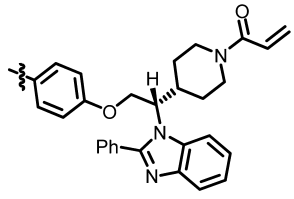	108 ± 18

[a]Affinities are measured by means of fluorescence polarization.

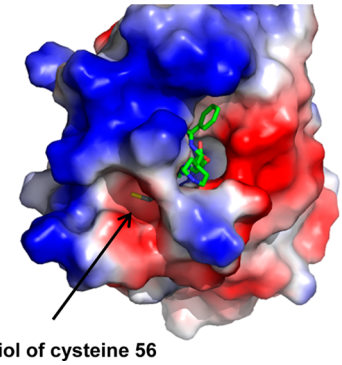

Figure 8. Orientation of the thiol function of cysteine 56. The thiol functionality points away from the inhibitor (PDB 4JVF).

(Scheme 5, Table 3). Indeed, replacement of the phenyl group in the guiding benzimidazole (*S*)-**54** with an isopropyl, an ethyl, or a cyclopropyl group yielded similarly potent compounds (Table 3, entries 2−4). However, the introduction of a methyl group resulted in reduced affinity.

In a further effort to decrease the size of the compounds, the substituent pointing toward cysteine 56 was eliminated in both the ester and the ether series. Surprisingly high affinity compounds were identified that bind with good ligand efficiency (Table 3, entries, 1−5). These data therefore suggest that a third hydrogen bond to cysteine 56 might not be necessary for the development of highly potent compounds targeting the K-Ras/PDEδ interaction. Analysis of the existing crystal structures does not provide any simple explanations for this finding. Biophysical experiments revealed that in the farnesyl bound state PDEδ is conformationally constrained compared with the free state, which results in an entropic penalty upon binding of ligands into the farnesyl cavity.[23] In addition PDEδ does not crystallize in the absence of bound ligands. Therefore, we believe that the interplay between the conformational restriction of PDEδ in the ligand bound state,[23] and the energetic cost of desolvation of the piperidine group might make the third hydrogen bond unnecessary for the ligands shown in Table 4.

dx.doi.org/10.1021/jm500632s | J. Med. Chem. XXXX, XXX, XXX−XXX

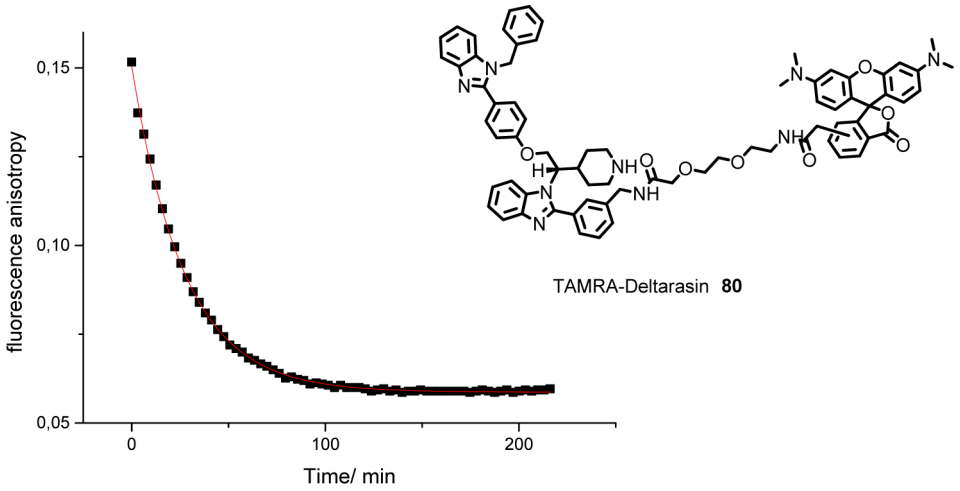

Figure 9. Representative competition experiment of TAMRA−deltarasin with an excess of (*S*)-**33** deltarasin observed by a fluorescence anisotropy time course. Conditions: TAMRA−deltarasin 33 nM, PDEδ 33 nM, and deltarasin 500 nM. Fit to single exponential function is shown.

Table 6. Characteristic Kinetic and Thermodynamic Data for the Interaction of Small Molecules with PDEδ as Determined by Means of Time-Resolved Fluorescence Anisotropy and Surface Plasmon Resonance (SPR) Measurements[a]

Entry	Compound	k_{on} / $M^{-1}s^{-1}$	k_{off} / s^{-1}	K_D/ nM
1	Dansyl-GKSSC(Far)-OMe from RheB	nd	3 #	102 #
2	TAMRA-Deltarasin **80**	nd	6.1×10^{-4}	7.6 #
3	TAMRA-(*S*)-**54**	nd	9.0×10^{-5}	5.3 #
4	**1**	3.9×10^{5}	0.9	2900* (2400)
5	(*S*)-**33** Deltarasin	6.3×10^{5}	6.9×10^{-4}	1.1*
6	(*S*)-**49**	8.6×10^{5}	6.5×10^{-5}	0.077*

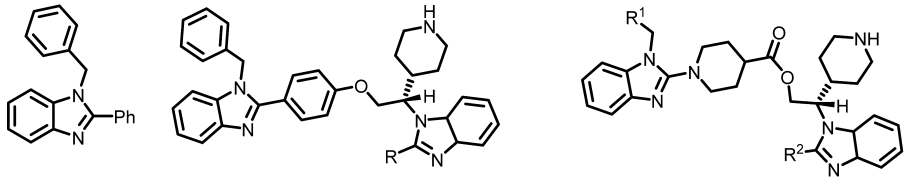

1

R= Ph
(*S*)-**33** Deltarasin

R= Linker-TAMRA
TAMRA-Deltarasin **80**

R^1= Ph R^2= Ph
(*S*)-**49**

R^1= 3-thienyl R^2= Linker-TAMRA
TAMRA-(*S*)-**54**

[a]The # indicates previously obtained values;[16,17,26] The * indicates K_D values for Biacore experiments derived from ratio of association and dissocation rate; data is based on three independent experiments. The value in parentheses is derived from steady-state analysis.

dx.doi.org/10.1021/jm500632s | *J. Med. Chem.* XXXX, XXX, XXX−XXX

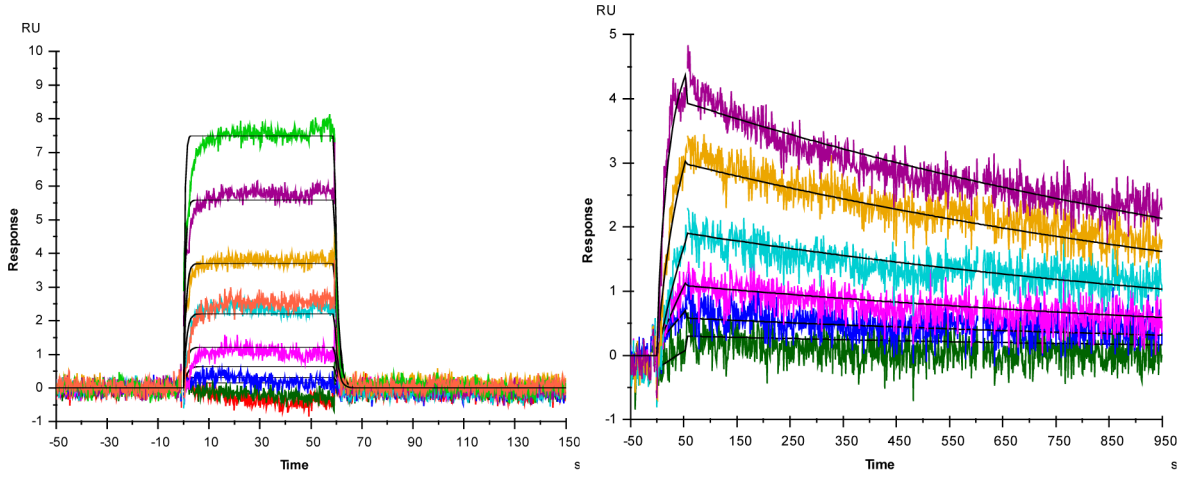

Figure 10. Representative SPR experiments carried out at 35 °C on a Biacore T100. For benzimidazole **1**, compound concentrations were varied from 63 to 8000 nM (left); for the bis-benzimidazole deltarasin, a concentration range of 2−64 nM was used (right). Time was measured in seconds.

The results shown in Table 4 indicate that potent inhibitors with reduced lipophilicity can be developed based on the bis-benzimidazole compounds. Bis-benzimidazole **74**, for example, has a molecular weight <500 Da and a predicted log *P* below 5.7. These improved features make compound **74** an interesting starting point for the synthesis of inhibitors with more drug-like properties. We also note that despite their lipophilicity bis-benzimidazoles can be formulated in emulsions for the use in mouse xenograft experiments.[16] The guiding bis-benzimidazole deltarasin, for example, showed antitumor activity against human pancreatic adenocarcinoma cells after intraperitoneal injection into mice.[16]

Attempted Targeting of Cysteine 56 with Covalent Inhibitors. Covalent inhibitors have recently found increasing application in drug discovery.[24] Irreversible, covalent inhibition can result in very long half-lives of the protein−ligand complexes *in vivo*. Therefore, covalent drugs often display increased residence times at the target of interest compared with noncovalent inhibitors. To explore the possibility of irreversible inhibitor binding to PDEδ, we investigated whether the formation of a covalent bond between a Michael acceptor and a cysteine residue is possible. Since PDEδ features only one cysteine close to the hydrophobic farnesyl binding cavity (cysteine 56, Figure 6), we equipped the benzimidazole inhibitors with reactive Michael acceptors (Table 5; for synthesis see the Supporting Information).

Unfortunately, none of the synthesized inhibitors showed significantly improved binding affinities compared with related nonreactive compounds. This finding can be attributed to the orientation of the thiol function of cysteine 56. Although PDEδ is very flexible, all cocrystal structures suggest that the thiol points out of the pocket and thus away from the inhibitor (Figure 8).

Kinetic Analysis of the Small Molecule−PDEδ Interaction. For efficient and tight ligand binding the rate constant k_{off} is of particular interest, because arguably k_{off} may be more predictive of biological activity than the equilibrium constant K_D.[25] Low dissociation rates of labeled small molecules can be determined by means of time-resolved fluorescence anisotropy measurements. In a standard assay setup with PDEδ, the TAMRA labeled small molecules were preincubated with the protein, and then a large excess of unlabeled competitor was added to determine the displacement of labeled compound in real time. When TAMRA−(*S*)-**54** and TAMRA−deltarasin **80** were used, the initially high fluorescence anisotropy decreased over time after addition of unlabeled deltarasin (Figure 9). Strikingly,

Table 7. Affinities of Atorvastatin Derivatives Determined by Means of Fluorescence Polarization

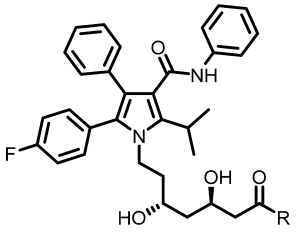

Entry	Compound	R	K_D / nM
1	**81**		1250 ± 234 [a)]
2	**82**	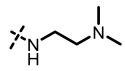	35 ± 9
3	**83**		16 ± 5
4	**84**	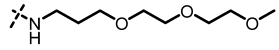	36 ± 15
5	**85**		26 ± 10

[a]Adopted from ref 16.

the rate constants for TAMRA−deltarasin k_{off} ($(6 \pm 1) \times 10^{-4}$ s^{-1}) and for TAMRA−(*S*)-**54** ($(9 \pm 5) \times 10^{-5}$ s^{-1}) are several orders of magnitude lower than the previously determined k_{off} of 3 s^{-1} for a farnesylated peptide mimicking the Ras-family protein RheB, which is also bound and shuttled in the cell by PDEδ (Table 6, entries 1−3).[26]

For competition of TAMRA−deltarasin with unlabeled small molecules and determination of the rate constant k_{off}, a labeled ligand is required, and the fluorophore may influence binding. Therefore, as an alternative label-free technique, surface plasmon resonance (SPR) was employed, which allows for the determination of affinities and kinetic parameters in a single experiment.[27,28] To this end, GST−PDEδ was reversibly immobilized on an anti-GST capturing surface. In these binding experiments, simple benzimidazole **1** showed a fast association and a fast

dx.doi.org/10.1021/jm500632s | J. Med. Chem. XXXX, XXX, XXX−XXX

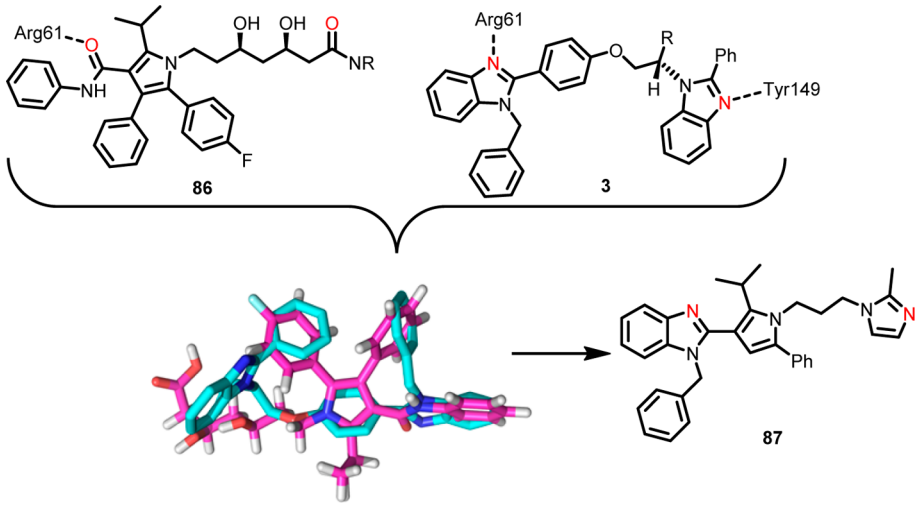

Figure 11. Design of hybrid atorvastatin−benzimidazole inhibitors. (top) Key hydrogen bond acceptors are highlighted. (bottom) Overlay of bis-benzimidazole (cyan) and atorvastatin (pink) from docking pose. In a hybrid approach, it was envisaged to keep the isopropyl substituted pyrrole moiety of atorvastatin, which according to docking extends into a hydrophobic pocket that was not targeted by the bis-benzimidazole compounds (compare with Figure 2).

Scheme 6. Synthesis of Benzimidazole/Pyrrole Hybrid Inhibitors

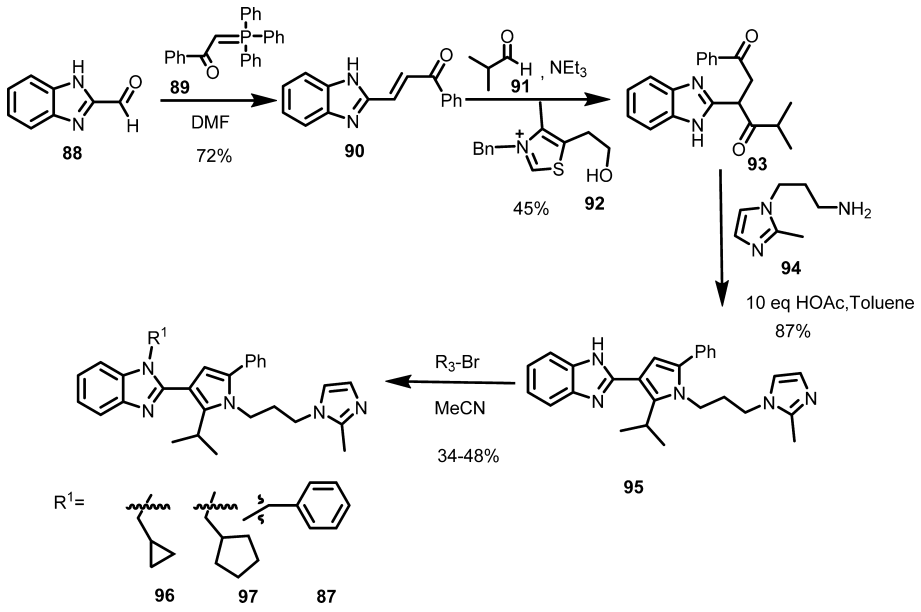

dissociation from immobilized PDEδ (Figure 10, left panel; Table 6, entry 4).

The association rates of the bis-benzimidazoles deltarasin and ester (*S*)-**49** are comparable (Figure 10, right panel; Table 6, entries 5 and 6). However, the dissociation rate, k_{off}, is strongly reduced for the more potent ligands (Table 6, entries 5 and 6). The dissociation rates k_{off} derived from SPR experiments agree well with the results obtained in the time-resolved fluorescence polarization measurements using labeled compounds (see above). The equilibrium constants K_D derived from the kinetic experiments are higher for the benzimidazole fragment **1**, whereas they are much lower for the bis-benzimidazoles deltarasin and ester (*S*)-**49**. Notably, according to these SPR experiments ester (*S*)-**49** binds with a very high affinity of 77 pM (Table 6, entry 5).

Synthesis of Atorvastatin Derivatives and Pyrrole−Benzimidazole Hybrid Inhibitors. The results obtained for the benzimidazoles demonstrate that the farnesyl binding site of PDEδ is druggable and allows for a continuous logical improvement of inhibitor structure. It is therefore to be expected that other inhibitor chemotypes may also be found and developed by analogy. To investigate this possibility, we drew form the previous qualitative finding that sildenafil derivatives and atorvastatin bind to PDEδ.[29−33] Since atorvastatin (K_D, 1250 nM, T_m shift 10.6 °C; Table 7, entry 1) proved to be a stronger binder than sildenafil (K_D > 5 μM, T_m shift 5.6 °C), a focused collection of atorvastatin derivatives was synthesized (Table 6), and the activity of these compounds as PDEδ inhibitors was investigated.

Notably, conversion of the carboxylic acid of atorvastatin into an amide (Table 7, entries 2−5) increased the affinity of the resulting pyrroles compared with atorvastatin itself by more than one order of magnitude. We reasoned that this striking increase in affinity could be explained by the change of the negatively charged carboxylate to a neutral amide and presumably formation of a second strong hydrogen bond to the amide. These atorvastatin

dx.doi.org/10.1021/jm500632s | J. Med. Chem. XXXX, XXX, XXX−XXX

Table 8. Affinities of Pyrrole–Benzimidazole Hybrid Compounds Measured by Fluorescence Polarization and T_m Shift Assays

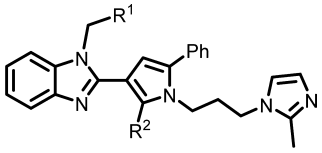

Entry	Cpd (rac)	R^1	R^2	K_D / nM	T_m shift / °C
1	**96**			251±33	18.3
2	**97**			347±47	19.6
3	**87**			689±223	nd

derivatives could potentially make two hydrogen bonds to Arg61 and Tyr149. Consistently, docking (Schrödinger, Maestro suite) of atorvastatin into the prenyl binding site of PDEδ showed an overlap of the anilide moiety of atorvastatin with a benzimidazole unit of the bis-benzimidazoles described above and formation of the hydrogen bond to Arg61.

According to the results obtained in the docking studies, the isopropyl substituted pyrrole moiety of atorvastatin extends into a hydrophobic pocket that was not targeted by the bis-benzimidazoles. It was thus attempted to combine the advantages of both compound classes into hybrid molecules that may result in more potent compounds with improved physicochemical properties (Figure 11). For the synthesis of these hybrid inhibitors 2-formyl benzimidazole was subjected to Wittig reaction resulting in an α,β-unsaturated ketone (Scheme 6). Stetter reaction with isopropyl carbaldehyde, followed by Paal–Knorr synthesis, furnished the benzimidazole–pyrrole core structure, and alkylation, as previously described, led to N-substituted benzimidazoles (Scheme 6).

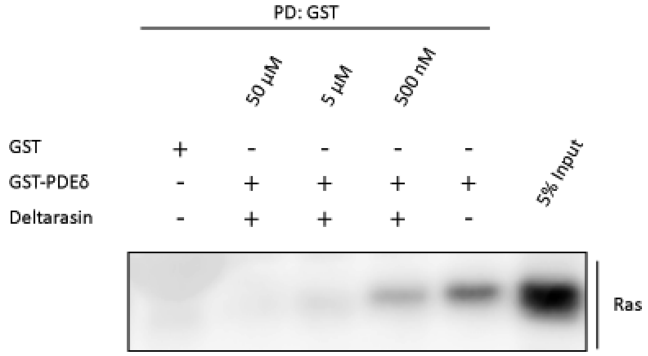

Figure 13. Pull-down experiments using immobilized GST–PDEδ. Western Blots were stained with an anti H/K-Ras anibody. For Ponceau staining of SDS-PAGE (GST-loading control), see Supporting Information.

However, as shown in Table 8, the resulting pyrrole–benzimidazole hybrid compounds did not show improved inhibitory potency toward PDEδ and are only modestly potent.

Target Engagement of Benzimidazoles with Endogenous PDEδ. With a series of very potent bis-benzimidazoles in hand, we investigated whether these compounds also bind to PDEδ in cell lysates. An excess of biotinylated deltarasin **98** was treated with magnetic beads coated with streptavidin, which were washed and then employed in affinity pull-down experiments with MDCK cell lysates (Figure 12). The fraction of PDEδ in the cell lysate that bound to the immobilized compounds was released from the beads by means of heating with SDS detergent. The resulting protein mixture was separated by SDS-PAGE and analyzed by Western blotting using an anti-PDEδ antibody. Immobilized deltarasin enriched PDEδ at the solid phase, which proves that the compound binds to endogenous PDEδ in cell lysates.

Additional validation was derived from independent competition experiments with varying concentrations of free deltarasin (Figure 12). The observation that free deltarasin competes with binding of PDEδ to immobilized ligand in a concentration-dependent

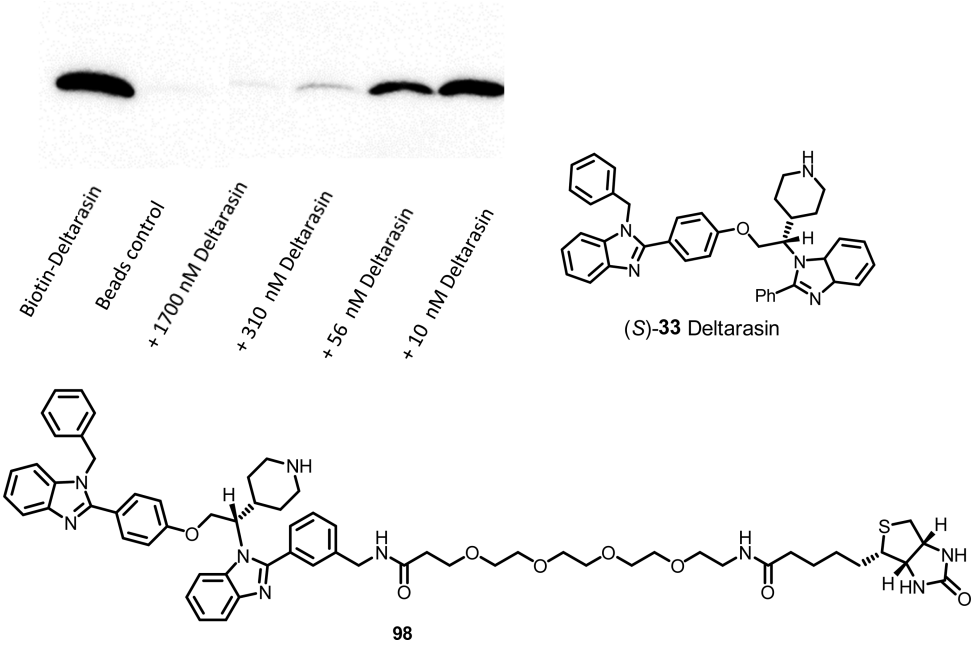

Figure 12. Pull-down experiments using immobilized bis-benzimidazole deltarasin in MDCK cells. Western blots were stained with anti-PDEδ antibody.

dx.doi.org/10.1021/jm500632s | J. Med. Chem. XXXX, XXX, XXX–XXX

manner further validated the interaction of both biotinylated and free deltarasin with PDEδ in MDCK cell lysates.

Inihibition of the Ras−PDEδ Interaction by Deltarasin. To characterize the interaction of deltarasin with PDEδ in human pancreatic adenocarcinoma cells, we analyzed the effect of deltarasin on the Ras−PDEδ interaction in oncogenic K-Ras dependent Panc-Tu-I cells.[34] GST−PDEδ was immobilized on magnetic beads and treated with Panc-Tu-I cell lysates. The fraction of endogenous Ras that bound to the immobilized GST−PDEδ was analyzed by means of SDS-PAGE and Western blot using an H/K-Ras specific antibody. GST−PDEδ clearly enriched Ras at the solid phase (Figure 13), and deltarasin decreased the amount of Ras−PDEδ complex on the solid phase in a dose-dependent manner. At compound concentrations as low as 500 nM, the amount of endogenous Ras at the solid phase was clearly decreased. These experiments with endogenous Ras clearly validate previous FRET−FLIM experiments in living cells using labeled Ras−PDEδ.[16]

CONCLUSION AND OUTLOOK

We have described the structure guided development of PDEδ inhibitors based on a bis-benzimidazole scaffold, which target the farnesyl binding pocket of PDEδ with nanomolar affinity. Our results demonstrate that the prenyl binding pocket of PDEδ is druggable and that logical, structure-guided design allows us to increase inhibitor potency and properties in a stepwise continuous manner. Our findings suggest that also other inhibitor classes with different scaffold structures and chemotypes may be developed following this structure guided approach. We have provided proof for this notion by the identification of potent atorvastatin derivatives. A detailed kinetic analysis of the interaction between potent bis-benzimidazoles and PDEδ revealed that off rates are at least 3 orders of magnitude lower than the rate constants k_{off} for farnesylated Ras-family proteins. Investigation of target engagement in cell lysates showed that bis-benzimidazoles like deltarasin bind at nanomolar concentrations to endogenous PDEδ.

ASSOCIATED CONTENT

Supporting Information

Detailed experimental procedures for biochemistry, cell biology, and chemical synthesis. This material is available free of charge via the Internet at http://pubs.acs.org.

AUTHOR INFORMATION

Corresponding Author

*E-mail: Herbert.Waldmann@mpi-dortmund.mpg.de. Phone +49 (231) 133-2400.

Notes

The authors declare no competing financial interest.

ACKNOWLEDGMENTS

The Compound Management und Screening Center (COMAS), Dortmund, is acknowledged for carrying out high-throughput screening and data analysis. G.Z. acknowledges the Fonds der Chemischen Industrie for a Kekulé Scholarship. We are grateful to Carsten Degenhart and Dr. Alexander Wolf, LDC, for help with initial Alpha screen assay development. Biaffin GmbH, Kassel, is acknowledged for carrying out SPR measurements. G.Z., C.S.F., G.T., S.I., A.W., and H.W. are inventors on a Max-Planck patent application concerning PDED inhibitors.

ABBREVIATIONS USED

ITC, isothermal titration calorimetry; DtBAD, di-*tert*-butyl azadicarboxylate; MDCK, Madin−Darby canine kidney; NMP, *N*-methyl pyrrolidone; PD, pull down; PDEδ, protein originally identified as δ-subunit of phosphodiesterase 6, prenyl binding protein; Ras, rat sarcoma (protein); SPR, surface plasmon resonance; TAMRA, tetramethylrhodamine; T_m, protein melting point; TMAD, *N*,*N*,*N*′,*N*′-tetramethylazodicarboxamide

REFERENCES

(1) Brunsveld, L.; Kuhlmann, J.; Alexandrov, K.; Wittinghofer, A.; Goody, R. S.; Waldmann, H. Lipidated ras and rab peptides and proteins-synthesis, structure, and function. *Angew. Chem., Int. Ed.* **2006**, *45*, 6622−6646.

(2) Prior, I. A.; Hancock, J. F. Ras trafficking, localization and compartmentalized signalling. *Semin. Cell Dev. Biol.* **2012**, *23*, 145−153.

(3) Wennerberg, K.; Rossman, K. L.; Der, C. J. The Ras superfamily at a glance. *J. Cell Sci.* **2005**, *118* (Pt 5), 843−846.

(4) Wang, W.; Fang, G.; Rudolph, J. Ras inhibition via direct Ras binding–is there a path forward? *Bioorg. Med. Chem. Lett.* **2012**, *22*, 5766−5776.

(5) Sun, Q.; Burke, J. P.; Phan, J.; Burns, M. C.; Olejniczak, E. T.; Waterson, A. G.; Lee, T.; Rossanese, O. W.; Fesik, S. W. Discovery of small molecules that bind to K-Ras and inhibit Sos-mediated activation. *Angew. Chem., Int. Ed.* **2012**, *51*, 6140−6143.

(6) Maurer, T.; Garrenton, L. S.; Oh, A.; Pitts, K.; Anderson, D. J.; Skelton, N. J.; Fauber, B. P.; Pan, B.; Malek, S.; Stokoe, D.; Ludlam, M. J.; Bowman, K. K.; Wu, J.; Giannetti, A. M.; Starovasnik, M. A.; Mellman, I.; Jackson, P. K.; Rudolph, J.; Wang, W.; Fang, G. Small-molecule ligands bind to a distinct pocket in Ras and inhibit SOS-mediated nucleotide exchange activity. *Proc. Natl. Acad. Sci. U. S. A.* **2012**, *109*, 5299−5304.

(7) Patgiri, A.; Yadav, K. K.; Arora, P. S.; Bar-Sagi, D. An orthosteric inhibitor of the Ras-Sos interaction. *Nat. Chem. Biol.* **2011**, *7*, 585−587.

(8) Lim, S. M.; Westover, K. D.; Ficarro, S. B.; Harrison, R. A.; Choi, H. G.; Pacold, M. E.; Carrasco, M.; Hunter, J.; Kim, N. D.; Xie, T.; Sim, T.; Jänne, P. A.; Meyerson, M.; Marto, J. A.; Engen, J. R.; Gray, N. S. Therapeutic targeting of oncogenic K-Ras by a covalent catalytic site inhibitor. *Angew. Chem., Int. Ed.* **2014**, *53*, 199−204.

(9) Ostrem, J. M.; Peters, U.; Sos, M. L.; Wells, J. A.; Shokat, K. M. K-Ras(G12C) inhibitors allosterically control GTP affinity and effector interactions. *Nature* **2013**, *503*, 548−551.

(10) Cho, K. J.; Park, J. H.; Piggott, A. M.; Salim, A. A.; Gorfe, A. A.; Parton, R. G.; Capon, R. J.; Lacey, E.; Hancock, J. F. Staurosporines disrupt phosphatidylserine trafficking and mislocalize Ras proteins. *J. Biol. Chem.* **2012**, *287*, 43573−43584.

(11) van der Hoeven, D.; Cho, K. J.; Ma, X.; Chigurupati, S.; Parton, R. G.; Hancock, J. F. Fendiline inhibits K-Ras plasma membrane localization and blocks K-Ras signal transmission. *Mol. Cell. Biol.* **2013**, *33*, 237−251.

(12) Rocks, O.; Peyker, A.; Kahms, M.; Verveer, P. J.; Koerner, C.; Lumbierres, M.; Kuhlmann, J.; Waldmann, H.; Wittinghofer, A.; Bastiaens, P. I. H. An acylation cycle regulates localization and activity of palmitoylated Ras isoforms. *Science* **2005**, *307*, 1746−1752.

(13) Nancy, V.; Callebaut, I.; El Marjou, A.; de Gunzburg, J. The delta subunit of retinal rod cGMP phosphodiesterase regulates the membrane association of Ras and Rap GTPases. *J. Biol. Chem.* **2002**, *277*, 15076−15084.

(14) Chandra, A.; Grecco, H. E.; Pisupati, V.; Perera, D.; Cassidy, L.; Skoulidis, F.; Ismail, S. A.; Hedberg, C.; Hanzal-Bayer, M.; Venkitaraman, A. R.; Wittinghofer, A.; Bastiaens, P. I. The GDI-like solubilizing factor PDEδ sustains the spatial organization and signalling of Ras family proteins. *Nat. Cell Biol.* **2012**, *14*, 148−158.

(15) Nikolova, S.; Guenther, A.; Savai, R.; Weissmann, N.; Ghofrani, H. A.; Konigshoff, M.; Eickelberg, O.; Klepetko, W.; Voswinckel, R.; Seeger, W.; Grimminger, F.; Schermuly, R. T.; Pullamsetti, S. S. Phosphodiesterase 6 subunits are expressed and altered in idiopathic pulmonary fibrosis. *Respir. Res.* **2010**, *11*, 146−159.

(16) Zimmermann, G.; Papke, B.; Ismail, S.; Vartak, N.; Chandra, A.; Hoffmann, M.; Hahn, S. A.; Triola, G.; Wittinghofer, A.; Bastiaens, P. I.; Waldmann, H. Small molecule inhibition of the KRAS-PDEδ interaction impairs oncogenic KRAS signalling. *Nature* **2013**, *497*, 638−642.
(17) Chen, Y. X.; Koch, S.; Uhlenbrock, K.; Weise, K.; Das, D.; Gremer, L.; Brunsveld, L.; Wittinghofer, A.; Winter, R.; Triola, G.; Waldmann, H. Synthesis of the Rheb and K-Ras4B GTPases. *Angew. Chem., Int. Ed.* **2010**, *49*, 6090−6095.
(18) Tsunoda, T.; Uemoto, K.; Nagino, C.; Kawamura, M.; Kaku, H.; Itô, S. A facile one-pot cyanation of primary and secondary alcohols. Application of some new Mitsunobu reagents. *Tetrahedron Lett.* **1999**, *40*, 7355−7358.
(19) Tempest, P.; Ma, V.; Thomas, S.; Hua, Z.; Kelly, M. G.; Hulme, C. Two-step solution-phase synthesis of novel benzimidazoles utilizing a UDC (Ugi/de-Boc/cyclize) strategy. *Tetrahedron Lett.* **2001**, *42* (30), 4959−4962.
(20) Meyer, E. A.; Castellano, R. K.; Diederich, F. Interactions with aromatic rings in chemical and biological recognition. *Angew. Chem., Int. Ed.* **2003**, *42* (11), 1210−50. Salonen, L. M.; Ellermann, M.; Diederich, F. Aromatic Rings in Chemical and Biological Recognition: Energetics and Structures. *Angew. Chem., Int. Ed.* **2011**, *50*, 4808−4842.
(21) Monovich, L. G.; Tommasi, R. A.; Fujimoto, R. A.; Blancuzzi, V.; Clark, K.; Cornell, W. D.; Doti, R.; Doughty, J.; Fang, J.; Farley, D.; Fitt, J.; Ganu, V.; Goldberg, R.; Goldstein, R.; Lavoie, S.; Kulathila, R.; Macchia, W.; Parker, D. T.; Melton, R.; O'Byrne, E.; Pastor, G.; Pellas, T.; Quadros, E.; Reel, N.; Roland, D. M.; Sakane, Y.; Singh, H.; Skiles, J.; Somers, J.; Toscano, K.; Wigg, A.; Zhou, S.; Zhu, L.; Shieh, W. C.; Xue, S.; McQuire, L. W. Discovery of potent, selective, and orally active carboxylic acid based inhibitors of matrix metalloproteinase-13. *J. Med. Chem.* **2009**, *52*, 3523−3538.
(22) Abad-Zapatero, C.; Metz, J. T. Ligand efficiency indices as guideposts for drug discovery. *Drug Discovery Today* **2005**, *10*, 464−469.
(23) Suladze, S.; Ismail, S.; Winter, R. Thermodynamic, Dynamic and Solvational Properties of PDEδ Binding to Farnesylated Cystein: A Model Study for Uncovering the Molecular Mechanism of PDEδ Interaction with Prenylated Proteins. *J. Phys. Chem. B* **2014**, *118*, 966−975.
(24) Singh, J.; Petter, R. C.; Baillie, T. A.; Whitty, A. The resurgence of covalent drugs. *Nat. Rev. Drug Discovery* **2011**, *10*, 307−317.
(25) Copeland, R. A.; Pompliano, D. L.; Meek, T. D. Drug-target residence time and its implications for lead optimization. *Nat. Rev. Drug Discovery* **2006**, *5*, 730−739.
(26) Ismail, S. A.; Chen, Y. X.; Rusinova, A.; Chandra, A.; Bierbaum, M.; Gremer, L.; Triola, G.; Waldmann, H.; Bastiaens, P. I.; Wittinghofer, A. Arl2-GTP and Arl3-GTP regulate a GDI-like transport system for farnesylated cargo. *Nat. Chem. Biol.* **2011**, *7*, 942−949.
(27) Frostell, A.; Vinterbäck, L.; Sjöbom, H. Protein-Ligand Interactions Using SPR Systems. *Methods Mol. Biol.* **2013**, *1008*, 139−165.
(28) Holdgate, G.; Geschwindner, S.; Breeze, A.; Davies, G.; Colclough, N.; Temesi, D.; Ward, L. Biophysical methods in drug discovery from small molecule to pharmaceutical. *Methods Mol. Biol.* **2013**, *1008*, 327−355.
(29) Chidley, C.; Haruki, H.; Pedersen, M. G.; Muller, E.; Johnsson, K. A yeast-based screen reveals that sulfasalazine inhibits tetrahydrobiopterin biosynthesis. *Nat. Chem. Biol.* **2011**, *7*, 375−383.
(30) Dadvar, P.; O'Flaherty, M.; Scholten, A.; Rumpel, K.; Heck, A. J. A chemical proteomics based enrichment technique targeting the interactome of the PDE5 inhibitor PF-4540124. *Mol. Biosyst.* **2009**, *5*, 472−482.
(31) Dadvar, P.; Kovanich, D.; Folkers, G. E.; Rumpel, K.; Raijmakers, R.; Heck, A. J. Phosphatidylethanolamine-binding proteins, including RKIP, exhibit affinity for phosphodiesterase-5 inhibitors. *ChemBioChem* **2009**, *10*, 2654−2662.
(32) Raijmakers, R.; Dadvar, P.; Pelletier, S.; Gouw, J.; Rumpel, K.; Heck, A. J. Target profiling of a small library of phosphodiesterase 5 (PDE5) inhibitors using chemical proteomics. *ChemMedChem* **2010**, *5*, 1927−1936.
(33) Lockhart, D. J.; Patel, H. K.; Milanov, Z. V.; Mehta, S. A.; Zarrinkar, P. P.; Biggs, W. H., III; Ciceri, P.; Fabian, M. A.; Treiber, D. K. Pyrrole compounds and uses thereof. US patent US 7323490 B2, 2004.
(34) Singh, A.; Greninger, P.; Rhodes, D.; Koopman, L.; Violette, S.; Bardeesy, N.; Settleman, J.; Gene, A. Expression Signature Associated with "K-Ras Addiction" Reveals Regulators of EMT and Tumor Cell Survival. *Cancer Cell* **2009**, *15*, 489−500.